Chinese Chemical Letters 31 (2020) 1792–1796

Contents lists available at ScienceDirect

Chinese Chemical Letters

journal homepage: www.elsevier.com/locate/cclet

Communication

Smart nanoprobe based on two-photon sensitized terbium-carbon dots for dual-mode fluorescence thermometer and antibacterial

Huicheng Yan[a], Hongyuhang Ni[b], Yiwei Yang[a], Changfu Shan[a], Xiaoxi Yang[a], Xiangkai Li[b,*], Jing Cao[a,*], Wenyu Wu[a], Weisheng Liu[a], Yu Tang[a,*]

[a] State Key Laboratory of Applied Organic Chemistry, Key Laboratory of Nonferrous Metal Chemistry and Resources Utilization of Gansu Province, College of Chemistry and Chemical Engineering, Lanzhou University, Lanzhou 730000, China
[b] Ministry of Education Key Laboratory of Cell Activities and Stress Adaptations, School of Life Sciences, Lanzhou University, Lanzhou 730000, China

ARTICLE INFO

Article history:
Received 6 November 2019
Received in revised form 4 December 2019
Accepted 12 December 2019
Available online 13 December 2019

Keywords:
Rare-earth
Fluorescence lifetime
Fluorescence intensity
Thermometer
Antibacterial

ABSTRACT

Accurate temperature measurement plays an important role in a variety of industrial processes and scientific researches. In our work, the dual-mode temperature response nanoprobe CDs-Tb-TMPDPA containing a two-photon ligand (4-(2,4,6-trimethoxyphenyl)-pyridine-2,6-dicarboxylic acid, TMPDPA) sensitized Tb^{3+} as a temperature-sensitive unit and carbon dots (CDs) as photothermal reagent and a fluorescence reference unit, have been designed and synthesized. In this system, both the fluorescence intensity ratio and the fluorescence lifetime have a good response to temperature. In addition, due to the excellent photothermal conversion capability of CDs, photothermal antibacterial ability was also tested. Based on the temperature dependence of the fluorescence and the two-photon excitation characteristics of CDs-Tb-TMPDPA, the nanoprobe can also be used in the anti-counterfeiting. Our finding opens a new prospect for the use of two-photon sensitized dual-mode fluorescence thermometers.

Temperature is a basic physical parameter of which accurate measurement is critical in a variety of industrial processes and scientific researches. Contact thermometers, which reflect the variation of the temperature by the touching between thermal probe and sample, are not suitable for fast moving objects or submicron temperature measurements [1]. Thus, it is urgent to develop new non-invasive and accurate thermometers that can achieve sub-micron temperature measurement. Fluorescent thermometers that indicate the temperature by fluorescence intensity or fluorescence lifetime is a promising alternative for sub-micron temperature measurement [2–5]. Compared to conventional organic fluorescent dyes, lanthanide ions have large Stokes shifts and ion-specific emission spectra [6,7]. In particularly, lanthanides exhibit very long decay times, so the differentiation of background autofluorescence (short life) and lanthanide optical signature signals can be easily achieved by using simple time-gating techniques. Considering the inherent chemical nature of the lanthanide ions, it is an outstanding candidate for achieving simultaneous indication temperature of fluorescence intensity ratio and fluorescence lifetime.

Overusing of antibiotics has made multi-drug resistant become more common. Therefore, antibiotic resistance is an important emerging health threat [8–10]. Hence, the development of new antibacterial drugs is extremely important. To the best of our Knowledge, proteins or DNA are extremely unstable to heat [11]. Thus, it is a promising treatment method that using light absorbing agents to convert light into heat energy that raises the temperature to degrade protein or DNA to kill bacteria. Compared to other photothermal reagents, such as gold nanoclusters and carbon nanomaterials [12–15], carbon dots (CDs) [16–20] have excellent optical absorption, photobleaching resistance, chemical stability, low toxicity and good biocompatibility. Thus, CDs are one of the best candidates for new antimicrobial agents. Based on above analyses, it will be fantastic to design a nano-intelligent probe, combining lanthanide ions with CDs, which can realize dual-mode temperature measurement and photothermal antibacterial.

In our work, we designed and synthesized the nanoprobe CDs-Tb-TMPDPA to achieve dual-mode temperature sensing and realize the potential information anti-counterfeiting and anti-bacterial capabilities (Scheme 1). In the nanoprobe, CDs was introduced to enhance the water solubility and increase biocompatibility. Moreover, as a temperature insensitive unit and photo-absorption agent, CDs had also been used to assist in monitoring temperature and photothermal ablation of bacterium. Then, Tb^{3+} ions were

* Corresponding authors.
E-mail addresses: xkli@lzu.edu.cn (X. Li), Caoj@lzu.edu.cn (J. Cao), tangyu@lzu.edu.cn (Y. Tang).

https://doi.org/10.1016/j.cclet.2019.12.022
1001-8417/

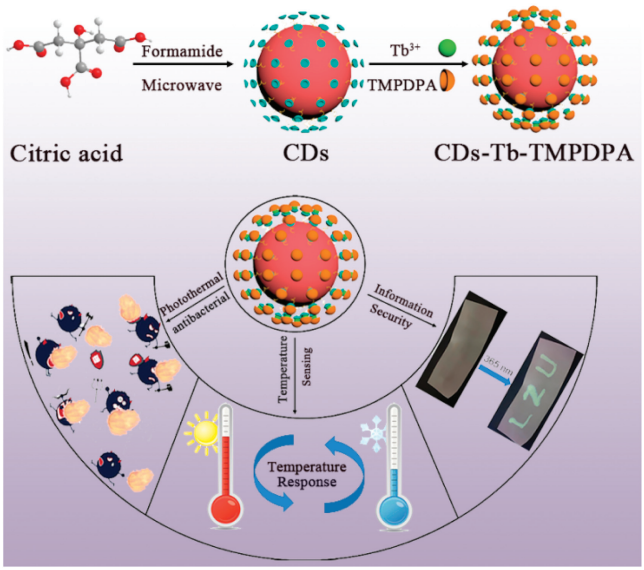

Scheme 1. Synthetic path of CDs-Tb-TMPDPA.

employed as thermosensitive unit. Because of the long emission lifetime and the significant change in fluorescence intensity of Tb^{3+}, it endowed the nanoprobe the ability to sense temperature in biology system. Finally, a two-photon ligand 4-(2,4,6-trimethoxyphenyl)-pyridine-2,6-dicarboxylic acid (TMPDPA) was coordinated with Tb^{3+}, cannot only achieve effectively sensitization of Tb^{3+}, but also avoid excitation light damage to normal tissues. Therefore, for the first time, we designed a smart two-photon-sensitized nanoprobe named CDs-Tb-TMPDPA, which can achieve dual-mode temperature sensing, and have information anti-counterfeiting and antibacterial capabilities.

First, the CDs-Tb-TMPDPA was synthesized. Slightly modified on the basis of the original synthesis [21]. Citric acid (2.8 g) was dissolved in 50 mL of formamide to obtain a clear solution. Thereafter, the above solution was transferred to an autoclave and placed in a microwave chemical reactor (warming procedure: 160 °C (400 W) for 1 h, 120 °C (400 W) for 1 h). After the reaction was completed, the autoclave was naturally cooled to room temperature. The solution was poured into an erlenmeyer flask and 250 mL of acetone was added and placed in a refrigerator (−20 °C) overnight. It was then filtered through a 0.45 μm filter to collect a solid. The product was then redispersed in methanol and centrifuged to remove large particles, the filtrate was collected, dialyzed, rotary evaporated and lyophilized to give a sample for further use. CDs (20 mg) and $Tb(NO_3)_3{\cdot}6H_2O$ (10 mg) were dissolved in 10 mL buffer solution (pH 7.4) and stirred at room temperature for 3 h. Then, a dimethyl sulfoxide solution of TMPDPA (2.5 mg/mL) was added dropwise to the reaction solution, and reacted at 25 °C for 3 h. After that the above reaction solution was dialyzed in distilled water with a cellulose ester dialysis membrane (2000 MWCO) for 2 days to remove "free" ligand and Tb^{3+} and then purified in a centrifuge (12,000 r/min, 5 min) to remove large or agglomerated particles. Thereafter, most of the water was removed by rotary evaporation and lyophilized to give a solid powder for further characterization and application.

The CDs-Tb-TMPDPA nanoparticles are dispersed in deionized water, and then ultrasonic treatment to obtain a uniform a fluorescent ink. Next, the brush was used to soak fluorescent ink to write LZU. The photothermal inhibition effect of CDs-Tb-TMPDPA was tested by using *E. coli* as a mold. Sterilized water containing CDs-Tb-TMPDPA or pure sterilized water was thoroughly mixed with 3 mL of *E. coli* solution. The above two control groups were irradiated with a 660 nm laser for 20 min (2 W/cm^2), abbreviated as black + light and black + M + light. The same two groups without any irradiation were set as the control group, respectively, and were abbreviated as black and black + M. The bacterial content in the two groups was measured by the colony forming unit (CFU) method. Each bacterial solution was diluted in a gradient. Each dilution was plated in triplicate and incubated for 12 h in LB medium. The control group and the material treatment group were compared to evaluate the inactivation effect.

Next, the nature of material was characterized. The prepared CDs are characterized with transmission electron microscopy (TEM) and dynamic light scattering (DLS) to confirm the morphology of nanoparticles. From Fig. 1a, we can see that CDs showed spherical shape, and embedded high-resolution transmission electron microscopy (HRTEM) image showed a *d* spacing values of 0.21 nm, which was close to the value of graphite carbon plane [22]. In Fig. 1b, the diameter of CDs ranged from 0.65 nm to 1.85 nm. There is no obvious change in the morphology of CDs after modification by the Tb^{3+} complex (Fig. S1 in Supporting information). The full scan X-ray photoelectron spectroscopy (XPS) image of the CDs (Fig. S2a in Supporting information) showed that the CDs contained C, O and N elements. The high resolution XPS further proved the existence of C—C/C=C, C—N, C—O/C=O, COOH and N—H bonds in CDs (Figs. S2b–d in Supporting information) [23]. The Fourier transform infrared (FTIR) spectrum (Fig. S3a in Supporting information) also proved the presence of C—N, C—O, C=O, C—N, —NH_2 and —OH bonds [24,25]. XPS and FTIR results showed that CDs had good water solubility and the potential of coordinating with Tb^{3+} ions.

The UV–vis absorption spectrum of CDs (Fig. 1c) displayed an extraordinarily broad absorption nearly crossing the whole UV–vis region, inferring that CDs can be used as a photo-absorption agent. And the synthesized CDs have typical excitation-dependent fluorescence property (Fig. 1d). The particle size unevenness of CDs and the surface state of CDs are the main causes that lead to the excitation-dependent fluorescence property of CDs [26,27]. Then, the effect of pH and illumination on CDs fluorescence was studied. As shown in Fig. S3b (Supporting information), the fluorescence intensity of the CDs was unchanged after continuous illumination of the UV lamp, indicating that the prepared CDs had good optical stability. As shown in Fig. S3c (Supporting information), the fluorescence intensity of CDs was changed slightly in the

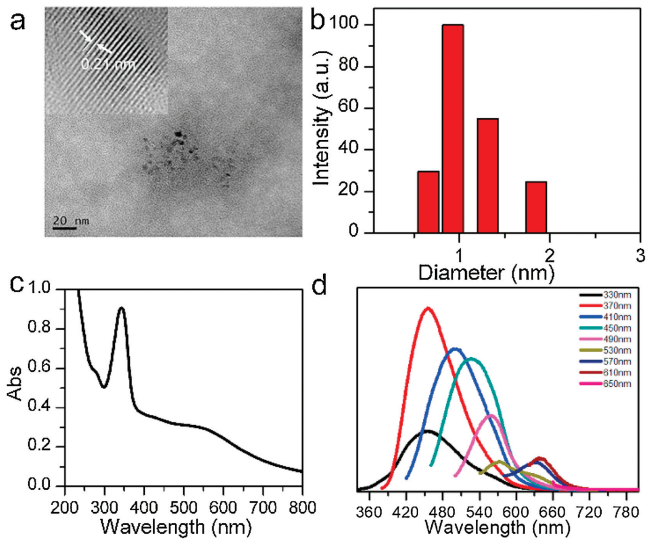

Fig. 1. (a) TEM images (insets showing HRTEM) of the CDs. (b) particles size distribution of CDs. (c) UV–vis absorption of CDs. (d) Fluorescence emission spectra of CDs with different excitation wavelengths.

pH range of 4–7.2, suggesting that the effect of pH on fluorescence was negligible.

The synthesis route of CDs-Tb-TMPDPA was shown in Scheme 1, CDs acted as ligands coordinated to Tb^{3+}, and then Tb^{3+} in CDs was further modification with the TMPDPA by a coordination effect. Finally, the obtained product CDs-Tb-TMPDPA provides both the thermometry and heater function. As shown in Fig. S4 (Supporting information), it was found that the emission intensity of CDs-Tb-TMPDPA linearly increased with the square of the laser power (using a 660 nm pulsed laser), which demonstrated a nature of the two-photon excited fluorescence process.

UV-vis spectrum, fluorescence emission spectrum, FTIR and XPS was further used to prove the chemical properties of CDs-Tb-TMPDPA. The nanoprobe exhibited absorption peaks of both CDs and the ligand TMPDPA with a little blue-shifted as shown in Fig. S5a (Supporting information). This may be attributed to the coordination of Tb^{3+} ions with both CDs and the ligand TMPDPA. As shown in Fig. S5b (Supporting information), the fluorescence emission of CDs-Tb-TMPDPA also displayed typical excitation wavelength dependent fluorescence. The fluorescence emission spectra of CDs-Tb were also tested. Compared to the CDs-Tb-TMPDPA, there was no characteristic fluorescence of Tb^{3+} by using the same excitation light that illustrated CDs could not sensitize Tb^{3+} (Fig. S5c in Supporting information). We next examined the fluorescence lifetime of CDs before and after modification. At 330 nm excitation, the average lifetime of the CDs is 10.36 ns, and after modification the average lifetime was 15.63 ns. These results indicated that the surface of the CDs was successfully modified with Tb^{3+} and TMPDPA.

XPS provided further evidence for the successful assembly of nanoprobe. It can be seen from Fig. S6a (Supporting information) that the CDs-Tb-TMPDPA probe showed a weak peak corresponding to Tb 4d. The high-resolution spectrum of Tb 3d (Fig. S6b in Supporting information) shows two peaks, corresponding to $3d_{5/2}$ (1241.4 eV) and $3d_{3/2}$ (1175.4 eV) of Tb^{3+}, respectively. It was further shown that the surface of the CDs was successfully functionalized with Tb^{3+}. The content of Tb^{3+} was determined to be 8.35% by inductively coupled plasma mass spectrometry. As shown in Fig. S6c (Supporting information), there was no peak of C = O in the infrared spectrum of CDs-Tb-TMPDPA, suggesting that CDs and TMPDPA successfully coordinates with Tb^{3+}. Next, the photostability of CDs-Tb-TMPDPA was studied. Fig. S7a (Supporting information) showed that CDs-Tb-TMPDPA had excellent photostability in 2 h. It can be seen from Figs. S7b and c (Supporting information) that both the fluorescence intensity ratio and the fluorescence lifetime change with pH. From the Fig. S7d (Supporting information), it can be deduced that metal ions have little effect on fluorescence intensity. Thus, the nanoprobe can be used in the biological system, and the information storage and anti-counterfeiting should be achieved through adjusting the fluorescence intensity and fluorescence lifetime by the acid-base stimuli of the CDs-Tb-TMPDPA.

Lanthanide ions present electronic states very close in energy in such a way that they are thermally coupled. The population distribution in thermally coupled states is strongly temperature-dependent, as it is controlled by Boltzmann statistics ($\exp(-E/kT)$, where k is the Boltzmann constant, T is the temperature, and E is the energy difference between the bottom of the excited state and the possibly non-radiative decay state), so that slight change in temperature will cause a related modification the population of the thermally coupled states [28,29]. Since the emission intensity produced by the electrons state is proportional to its population, wherefore temperature change can be monitored by exploiting the emission intensity produced by the thermally coupled state, thereby allowing the temperature to be measured. Next, the response of fluorescence intensity ratio to temperature was measured. As shown in Fig. 2a, upon temperature increasing, the emission intensity of $^5D_4$-$^7F_5$ transition (I_{546}) was descended, but the emission of CDs (I_{444}) was almost unchanged, which displayed temperature-dependent spectral dropped. The relationship between temperature and I_{546}/I_{444} can be fitted as a function of Eq. 1:

$$I_{546}/I_{444} = 6.473\text{-}0.0733\,T \quad (1)$$

with a correlation coefficient (R^2) of 0.98 (Fig. 2b). Fig. 2c showed that the maximum relative sensitivity was 3.49%/°C at 60 °C.

From previously reports [30,31], we notice that unlike the fluorescence intensity, the fluorescence lifetime value is not affected by the intensity fluctuations of light scattering, reflection or excitation sources. Thus, the response of fluorescence lifetime to temperature was measured. Fig. 2d showed the decay curves of CDs-Tb-TMPDPA. The temperature dependence of the fluorescence

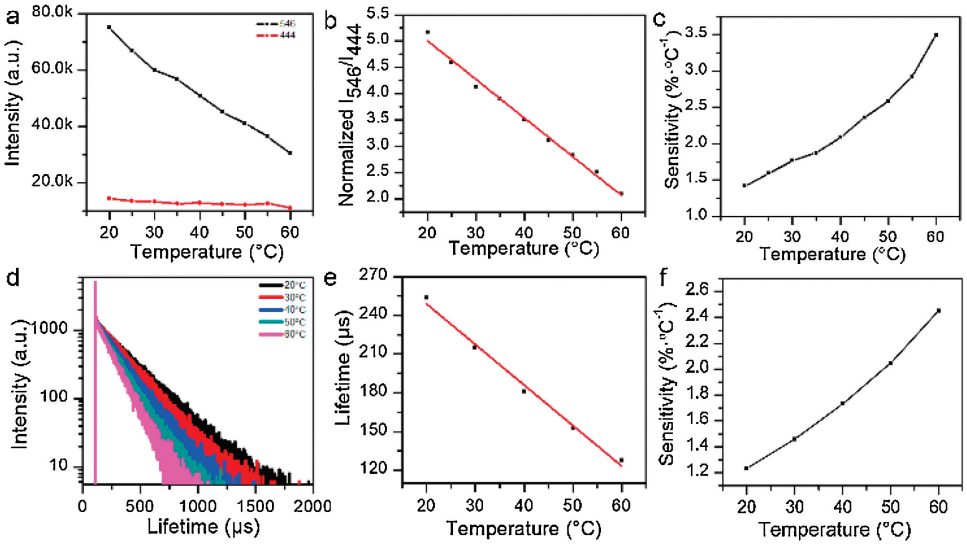

Fig. 2. (a) Temperature-dependent intensity of 546 nm and 444 nm transitions under 330 nm excitation. (b) Intensity ratio I_{546}/I_{444} of CDs-Tb-TMPDPA and the fitted curve. (c) The relative sensitivity (Sr) for CDs-Tb-TMPDPA. (d) The fluorescence lifetime fit map of CDs-Tb-TMPDPA. (e) Temperature-dependent lifetime data of CDs-Tb-TMPDPA and the fitted curve. (f) The relative sensitivity (Sr) of temperature-dependent lifetime for CDs-Tb-TMPDPA.

lifetime was shown in Fig. 2e. The relationship between luminescence lifetime and temperature corresponds to this Eq. 2:

$$\Delta = 311.398 - 3.133T \quad (2)$$

with correlation coefficient 0.98, where Δ represent lifetime of $^5D_4$-$^7F_5$ and T is the temperature. From 20 °C to 60 °C, the fluorescence lifetime of CDs-Tb-TMPDPA was decreased from 253 μs to 127 μs. Long fluorescence lifetime lead to a high degree of differentiation from short-lived autofluorescence. Thence, it can effectively deduct the interference of small molecules in biological systems. And the maximum sensitivity of CDs-Tb-TMPDPA NPs was determined to be 2.45%/°C at 60 °C (Fig. 2f). As shown in Table S1 (Supporting information), compared to the published systems with fluorescence lifetime as a temperature indicating parameter, CDs-Tb-TMPDPA has a relatively high sensitivity and has potential for application in biological systems.

Next, we used a digital frequency domain technique called FastFLIM in combination with a phasor map to further investigate the CDs-Tb-TMPDPA fluorescence lifetime. The phasor diagram is an effective method of life data analysis [32,33]. It converts the phase (f) and modulation (m) measurements in the frequency domain into phasor spaces (G, S), making the original lifetime measurements directly located on the 2D phasor diagram. Thus, the lifetime data can be described and analysed on a two-dimensional graph. As shown in Fig. 3a, it displayed that the fluorescence lifetime was significantly decreased as the temperature increases. Moreover, the fluorescence lifetime corresponding to each temperature can be directly acquired from the plot. In addition, the pseudo-color map of lifetime (Fig. 3b) can more intuitively reflect the trend of fluorescence lifetime with temperature.

One of the most important capabilities of CDs-Tb-TMPDPA is the NIR light-induced thermal effect, which can be used in photothermal antibacterial. First, the effect of concentration on the photothermal effect was studied. The sample was irradiated with 660 nm NIR laser (2 W/cm^2) for 10 min. Upon NIR irradiation, the CDs-Tb-TMPDPA solutions prepared displayed a gradual temperature increase with time (Fig. S8a in Supporting information). In addition, it was found that the materials showed a concentration-dependent temperature increasing. Furthermore, after 10 min of irradiation, the temperature of the CDs-Tb-TMPDPA solution (0.3 μg/mL) was raised from 26.3 °C to 58.5 °C. In contrast, the temperature of pure water was almost constant under the same conditions. From Fig. S8b (Supporting information), it inferred that laser power affected the thermal effects of CDs-Tb-TMPDPA. Finally, it was found that the heat generation ability of CDs-Tb-TMPDPA was almost unchanged in the repeated experiments, indicating that CDs-Tb-TMPDPA has good photothermal stability (Fig. S7c in Supporting information). Therefore, CDs-Tb-TMPDPA has potential as a new antimicrobial agent.

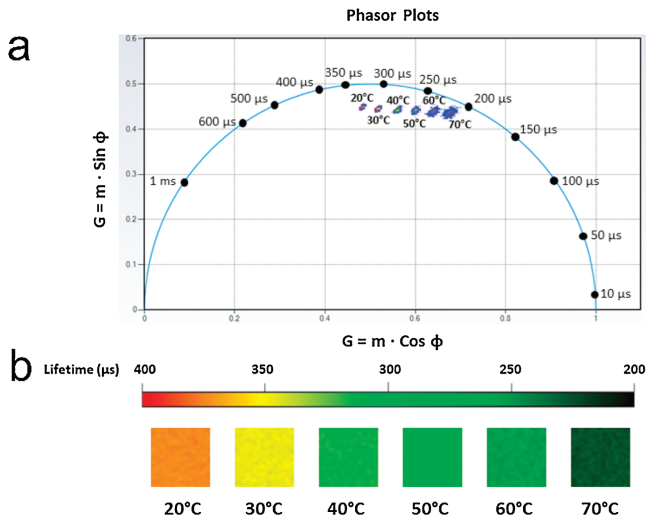

Fig. 3. (a) The phasor plot (semicircle plot) of CDs-Tb-TMPDPA. (b) Pseudocolor luminescence lifetime images of CDs-Tb-TMPDPA at temperatures between 20 °C and 70 °C. The orange red ("high lifetime") corresponds to a lifetime of 400 μs, the color dark green to 200 μs.

The application of terbium functionalized nanoprobes was investigate. As shown in the Fig. S9a (Supporting information), it was observed that the green light was gradually weakened with temperature increased, which indicated that the fluorescence intensity is affected by temperature. Then, an aqueous solution of CDs-Tb-TMPDPA was used as an ink, and letters "LZU" was written on the filter paper. As shown in Fig. S9b (Supporting information), there was no significant change under visible light, and it showed green fluorescence under the illumination of 365 nm UV lamp. Therefore, CDs-Tb-TMPDPA has the potential to sense temperature and may be used in information anti-counterfeiting. And the fluorescence intensity of the letters should be changed by the stimuli of the external temperature. And the fluorescence of the probe can be excited by the wavelength of 330 nm and 660 nm. These all should be keys to decode, thus the anti-counterfeiting level of this probe can be very high.

The photothermal inhibition ability of the material was tested. The *E. coli* solution or *E. coli* solution containing CDs-Tb-TMPDPA was irradiated with a 660 nm laser for 20 min (2 W/cm^2), abbreviated as black + light and black + M + light, respectively. The same two groups without any irradiation were set as the control group, and were abbreviated as black and black + M. As can be seen from Fig. S9c (Supporting information), the survival rates of the black and black + light groups were almost the same, indicating that illumination is useless when no material is added. From the XPS results, we knew that nanoprobes can be used as carbon sources. Therefore, the activity of *E. coli* was increased after the addition of the material [34]. And the group of black + M + light showed the mortality rate of *E. coli* was as high as 98.82%. This suggested that CDs-Tb-TMPDPA has excellent photothermal antibacterial ability and can be used as a new type of antibacterial agent in the antibacterial area.

In summary, we have successfully developed a smart two-photon sensitized nanoprobe CDs-Tb-TMPDPA, which can simultaneously achieve temperature sensing and optical heating. When the temperature is indicated by the fluorescence intensity ratio, the maximum sensitivity of the nanoprobe is 3.49%/°C. In addition, the fluorescence lifetime of Tb^{3+} decreased from 253 μs to 127 μs with the temperature increase, and the maximum sensitivity was as high as 2.45%/°C. Thus, the CDs-Tb-TMPDPA nanoprobe can be considered as an ideal candidate to achieve real-time temperature response. As an excellent photothermal bacteriostatic agent, CDs-Tb-TMPDPA can kill bacteria by converting light energy into heat under 660 nm irradiation. In addition, the probe can be used in the fluorescence anti-counterfeiting based on the temperature-dependence fluorescence and dual excitation wavelength. Thus, the design of the smart two-photon sensitized CDs-Tb-TMPDPA nanoprobe supplies a distinguished strategy of utilizing two-photon ligand sensitization and CDs as a host matrix to enhance the property of probe for synchronous temperature sensing, anti-counterfeiting and antibacterial.

Declaration of competing interest

The authors declare that they have no known competing financial interests or personal relationships that could have appeared to influence the work reported in this paper.

Acknowledgments

We acknowledge the National Natural Science Foundation of China (Nos. 21871121, 21801104 and 21601074) and Fundamental Research Funds for the Central Universities (No. Lzujbky-2018-ot01). The authors also thanks to the ISS Company and Dr. Hailin Qiu for their assistance in providing FastFLIM imaging.

Appendix A. Supplementary data

Supplementary material related to this article can be found, in the online version, at doi:https://doi.org/10.1016/j.cclet.2019.12.022.

References

[1] Y.J. Cui, F.L. Zhu, B.L. Chen, G.D. Qian, Chem. Commun. 51 (2015) 7420–7431.
[2] H.C. Yan, H.Y.H. Ni, Y. Tang, et al., Anal. Chem. 91 (2019) 5225–5234.
[3] Q. Zhu, S.Y. Li, J.F. Jin, et al., Chem.-Asian. J. 13 (2018) 3664–3669.
[4] Q. Zhu, J.J. Liu, X.D. Li, X.D. Sun, J.G. Li, Appl. Surf. Sci. 489 (2019) 142–148.
[5] Q. Zhu, S.Y. Li, Q. Wang, et al., Nanoscale 11 (2019) 2795–2804.
[6] P.C. de Sousa, J. Alain, G. Lemenager, et al., J. Phys. Chem. C 123 (2019) 2441–2450.
[7] H.C. Aspinall, Chem. Rev. 102 (2002) 1807–1850.
[8] L.N. Silva, K.R. Zimmer, A.J. Macedo, D.S. Trentin, Chem. Rev. 116 (2016) 9162–9236.
[9] M. Garland, S. Loscher, M. Bogyo, Chem. Rev. 117 (2017) 4422–4461.
[10] A. Bunschoten, M.M. Welling, M.F. Tennaat, M. Sathekge, F.W.B. van Leeuwen, Bioconjugate Chem. 24 (2013) 1971–1989.
[11] H. Suo, X.Q. Zhao, Z.Y. Zhang, C.F. Guo, ACS Appl. Mater. Interfaces 9 (2017) 43438–43448.
[12] L. Gao, J.B. Fei, J. Zhao, et al., ACS Nano 6 (2012) 8030–8040.
[13] C. Liang, S. Diao, C. Wang, et al., Adv. Mater. 26 (2014) 5646–5652.
[14] W.Q. Wang, L. Wang, Y. Li, et al., Adv. Mater. 28 (2016) 9320–9325.
[15] N. Li, Q.Q. Sun, Z.Z. Yu, et al., ACS Nano 12 (2018) 5197–5206.
[16] Y.S. Ma, Y. Cen, M. Sohail, et al., ACS Appl. Mater. Interfaces 9 (2017) 33011–33019.
[17] H.F. Liu, Y.Q. Sun, Z.H. Li, et al., Chin. Chem. Lett. 30 (2019) 1647–1651.
[18] X. Geng, Y.Q. Sun, Z.H. Li, et al., Small 15 (2019) 1901517.
[19] X.X. Shi, H.M. Meng, Y.Q. Sun, et al., Small 15 (2019) 1901507.
[20] H.F. Liu, Y.Q. Sun, J. Yang, et al., Sens. Actuators. B -Chem. 280 (2019) 62–68.
[21] S. Sun, L. Zhang, K. Jiang, A.G. Wu, H.W. Lin, Chem. Mater. 28 (2016) 8659–8668.
[22] J. Tang, B. Kong, H. Wu, et al., Adv. Mater. 25 (2013) 6569–6574.
[23] L.L. Pan, S. Sun, A.D. Zhang, et al., Adv. Mater. 27 (2015) 7782–7787.
[24] F. Arcudi, L. Dordevic, M. Prato, Angew. Chem. Int. Ed. 55 (2016) 2107–2112.
[25] D. Qu, M. Zheng, P. Du, et al., Nanoscale 5 (2013) 12272–12277.
[26] J. Jiang, Y. He, S.Y. Li, H. Cui, Chem. Commun. 48 (2012) 9634–9636.
[27] S.C. Ray, A. Saha, N.R. Jana, R. Sarkar, J. Phys. Chem. C 113 (2009) 18546–18551.
[28] C.D.S. Brites, P.P. Lima, N.J.O. Silva, et al., Nanoscale 4 (2012) 4799–4829.
[29] B. del Rosal, E. Ximendes, U. Rocha, D. Jaque, Adv. Opt. Mater. 5 (2017) 1600508.
[30] J.Y. Wang, J. Xue, Z.H. Yan, et al., Angew. Chem. Int. Ed. 56 (2017) 14928–14932.
[31] E. Baggaley, M.R. Gill, N.H. Green, et al., Angew. Chem. Int. Ed. 53 (2014) 3367–3371.
[32] Y.S. Sun, R.N. Day, A. Periasamy, Nat. Protoc. 6 (2011) 1324–1340.
[33] N.C. Shaner, G.G. Lambert, A. Chammas, et al., Nat. Methods 10 (2013) 407–409.
[34] J.A. Cotruvo, E.R. Featherston, J.A. Mattocks, J.V. Ho, T.N. Laremore, J. Am. Chem. Soc. 140 (2018) 15056–15061.